The Journal of Navigation (2021), **74**:5 1009–1025
doi:10.1017/S0373463321000400

CAMBRIDGE UNIVERSITY PRESS

RESEARCH ARTICLE

A new underwater positioning model based on average sound speed

Yixu Liu,[1] Xiushan Lu,[1] Shuqiang Xue,[2] and Shengli Wang[1]*

[1] Shandong University of Science and Technology, Qingdao, China.
[2] Chinese Academy of Surveying and Mapping, Beijing, China.
*Corresponding author. E-mail: shlwang@sdust.edu.cn

Received: 9 September 2020; **Accepted:** 8 April 2021; **First published online:** 20 May 2021

Keywords: underwater positioning, average sound speed, sound speed profile, incident angle

Abstract

The layout of seafloor datum points is the key to constructing the seafloor geodetic datum network, and a reliable underwater positioning model is the prerequisite for achieving precise deployment of the datum points. The traditional average sound speed positioning model is generally adopted in underwater positioning due to its simple and efficient algorithm, but it is sensitive to incident angle related errors, which lead to unreliable positioning results. Based on the relationship between incident angle and sound speed, the sound speed function model considering the incident angle has been established. Results show that the accuracy of positioning is easily affected by errors related to the incident angle; the new average sound speed correction model based on the incident angle proposed in this paper is used to significantly improve the underwater positioning accuracy.

1. Introduction

Marine navigation, positioning and the development of marine resources are increasingly of concern for most countries around the world. Research on underwater navigation and positioning technology has become increasingly mature (Yang et al., 2020). The construction of the submarine geodetic reference network is extremely difficult, and the technical requirements for the calibration of reference points are rigorous. Hence, more precise underwater positioning is required. The GNSS-A system uses acoustic technology to achieve underwater positioning, assisted by global navigation satellite system (GNSS) positioning on the sea surface, consequently completing the joint measurement of land and ocean space positions (Fujita et al., 2006). However, due to the particularity of the water environment, underwater positioning has the characteristics of being dynamic and non-repeatable compared with land positioning. Under the current observation conditions, the time measurement error can be controlled to within 0·1 ms (Zhao et al., 2018). Thus, the sound speed error is the main factor affecting the positioning accuracy. The traditional calculation of straight-line distance is based on the assumption that the sound speed is a constant in the water. Actually, the sound speed is a complex function of temperature, salinity and pressure, which have strong temporal and spatial characteristics (Liu et al., 2020). The change of sound speed with depth is expressed by the sound speed profile (SSP). SSP measurement is generally obtained by direct measurement using the 'underwater sound speed meter' (Jamshidi and Abu Bakar, 2010). Munk proposed the now classic Munk-SSP model, which is suitable for the deep sea, based on the stratification characteristics of the density structure of the measured deep sea (Munk, 1974). The acoustic ray bending error is caused by the refraction of sound waves during the propagation process due to the change of sound speed, and the propagation of sound signals obeys Snell's law (Zhao et al., 2009).

© The Author(s), 2021. Published by Cambridge University Press on behalf of The Royal Institute of Navigation

https://doi.org/10.1017/S0373463321000400 Published online by Cambridge University Press

Zhao's research shows that sound speed error is the main source of error in underwater positioning, and cannot be ignored in high-precision positioning (Zhao et al., 2019). Therefore, the correction of the sound speed is one of the key technologies to improve the accuracy of underwater acoustic positioning.

The average sound speed positioning model directly uses a single sound speed for distance measurement. This model is simple and efficient, but it ignores the effect of sound speed errors. Based on the Taylor series expansion, a sound speed correction method through numerical simulation has been proposed, which is suitable for different SSP. However, when the elevation angle is small, the sound speed error is larger (Li, 2015). The empirical sound speed method can quickly calculate the sound speed, but it requires a large amount of experimental research, and the determination of coefficients is complicated (Zhao et al., 2008). Others have proposed to use a neural network method for sound speed correction, but the model and method are not mature enough – follow-up research is still needed. Vincent and Hu (2000) put forward the concept of effective sound speed based on ray theory. To meet the real-time performance of the positioning system, a two-dimensional table of water depth and pitch angle is established to achieve rapid acquisition of sound speed. However, the process of establishing the table requires extensive calculation and storage space. Ray tracing technology uses the layer addition method to calculate the acoustic ray propagation path. Based on the accurate measurement of sound speed, it reduces the influence of the acoustic ray bending error to obtain high-precision three-dimensional coordinates of underwater target points (Sakic et al., 2018; Wang et al., 2009). The processing of residual information is also very important for the analysis of positioning accuracy, and a cubature Kalman filter with a multi-rate residual correction algorithm is proposed to fuse inertial navigation systems (INS) and polarization compass (PC) navigation outputs with different sampling frequencies (Zhao et al., 2020). The accuracy of the above algorithm is higher than that of the average sound speed positioning model, however, it also has problems, such as complex positioning model and low calculation efficiency (Sun, 2007).

Incident angle related errors are an important error source in positioning, including ranging system noise errors, sound speed errors and control point errors. Studies have shown that the impact of sound speed on distance measurement and positioning is related to the beam incident angle and depth, which is significant and cannot be ignored (Zhao et al., 2019). Therefore, when the observation configuration is not good, the range of incident angle is large, and the error of the average sound speed model has a significant influence, leading to inaccurate positioning results. The motivation of this research is to improve the efficiency of the solution without losing, or only slightly reducing, the accuracy. This paper introduces the principle of the underwater geometric positioning solution based on the average sound speed, and gives the method of calculation of the average sound speed. On this basis, considering the influence of the incident angle related error, a new sound speed positioning model related to the incident angle is established. The effectiveness of the algorithm is verified through experiments. The contribution of this research is to help to realise the positioning of underwater targets quickly, and the positioning accuracy will also be guaranteed. The rapid positioning of underwater targets will help the rapid establishment of seafloor datum points and the monitoring of underwater moving targets, such as submersibles and underwater robots.

2. Theoretical backgrounds

2.1. Mathematical model of geometric position of average sound speed

GNSS-A technology links GNSS and acoustic positioning methods to co-locate to accurately locate the position of the seafloor datum point. As shown in Figure 1, the transducer is installed under the ship and performs active ranging and positioning during the voyage, forming N sea-level dynamic control points within a period of time. Using GNSS technology can accurately determine their three-dimensional (3D) coordinates. When there are multiple distance observations, the 3D position information of the target point can be obtained through the distance intersection method (Sun, 2007). The underwater positioning

https://doi.org/10.1017/S0373463321000400 Published online by Cambridge University Press

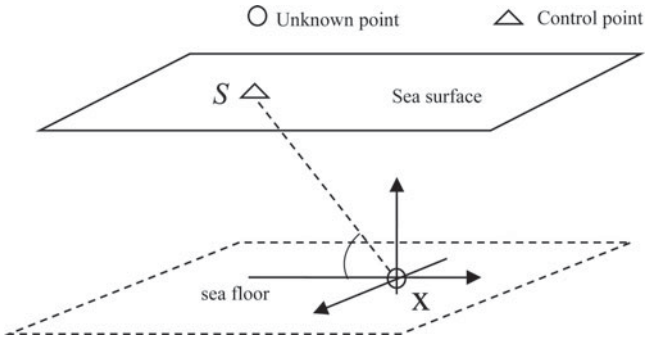


Figure 1. *GNSS/acoustic positioning local coordinate system.*

observation model based on the average sound speed is:

$$L^s = v^s t^s = ||\mathbf{x} - \mathbf{x}^s||_2 + \varepsilon_L \quad s \in \{1, 2, \ldots, N\} \tag{1}$$

where L^s is the propagation distance of the acoustic signal from the sea surface transducer to the transponder; v^s is average sound speed; t^s is the propagation time; $||\mathbf{x} - \mathbf{x}^s||_2$ is the Euclidean distance between two points; ε_L is the equivalent ranging error; N represents the number of sea surface movement control points.

Carry out the Taylor series expansion of Equation (1) at the initial value $\mathbf{x}_0$ to obtain the linearised equation:

$$dL^s = \mathbf{e}_i \mathbf{d}x + r_i + \varepsilon \tag{2}$$

where $\mathbf{d}x = \mathbf{x} - \mathbf{x}_0$ is coordinate correction number; r_i is the linearisation residual term, which can generally be ignored;

$$\mathbf{e}_i = (\mathbf{x}_0 - \mathbf{x}_i)/d_i(\mathbf{x}_0) \tag{3}$$

$\mathbf{e}_i$ is the direction cosine. When there are three or more observations, the adjustment criterion is introduced, and the least square solution can be expressed as:

$$\mathbf{d}\hat{\mathbf{x}} = (\mathbf{J}^T \mathbf{P} \mathbf{J})^{-1} \mathbf{J}^T \mathbf{P} \mathbf{b} \tag{4}$$

where $\mathbf{P} = \begin{bmatrix} \mathbf{P}_1 & \ldots & \mathbf{P}_n \end{bmatrix}$ is the observation weight matrix; $\mathbf{b} = \begin{bmatrix} dL_1 & dL_2 & \cdots & dL_n \end{bmatrix}$; $\mathbf{J} = \begin{bmatrix} \mathbf{J}' & \mathbf{k}_n \end{bmatrix}$ is called Jacobi matrix:

$$\mathbf{J} = \begin{bmatrix} \mathbf{e}_1^T & \mathbf{e}_2^T & \cdots & \mathbf{e}_n^T \end{bmatrix} \quad \mathbf{k}_n = \begin{bmatrix} 1 & \cdots & 1 \end{bmatrix}^T \tag{5}$$

$\mathbf{k}$ is the column matrix with a content of 1. Based on the initial value $\mathbf{x}_0$, the coordinates of the underwater point to be measured can be calculated iteratively:

$$\hat{\mathbf{x}} = \mathbf{x_0} + \mathbf{d}\hat{\mathbf{x}} \tag{6}$$

From the range-finding underwater positioning model, we can see that the sound speed is the most important parameter, and the selection of the sound speed directly determines whether the positioning result is reliable. Therefore, a lot of research and analysis have been done on the sound speed correction method in order to improve the accuracy of sonar underwater positioning.

2.2. Description of average sound speed

In the underwater positioning model, the range is determined by the sound speed and the propagation time. Currently, the time measurement error is generally within 0·1 ms (Zhao et al., 2018). Therefore,

https://doi.org/10.1017/S0373463321000400 Published online by Cambridge University Press

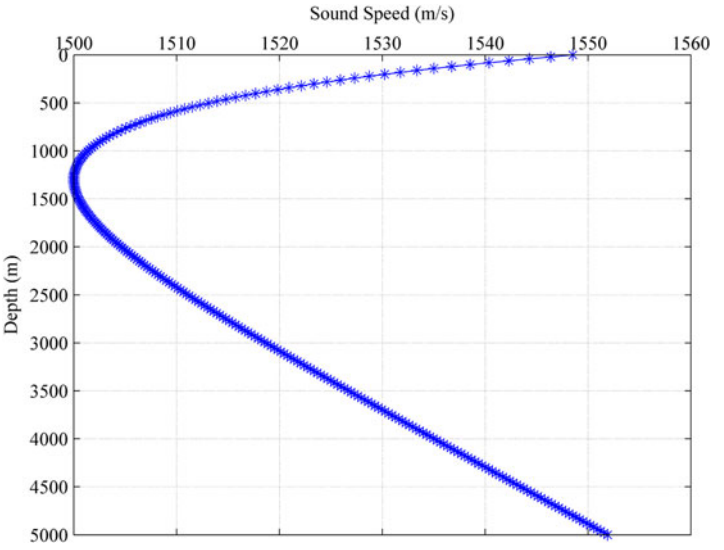


Figure 2. *Classic Munk sound speed profile.*

the key to improving the positioning accuracy lies in the determination of the sound speed. The equation of state of sea water (Cai et al., 2012) is:

$$dp = v^2 d\rho \tag{7}$$

where ρ is the density at a certain point i in seawater; p is the instantaneous sound pressure at the same point; v is the sound speed which can be expressed as:

$$v = \sqrt{dp/d\rho} = 1/\sqrt{\rho\beta} \tag{8}$$

The three influencing factors mainly change with the depth direction, so the sound speed can be roughly expressed as a function of water depth, and the relationship between them is expressed by the SSP. The SSP can be measured by CTD (conductivity, temperature, depth) or calculated according to the sound speed experience model. The water environment in the ocean is relatively complex, and temperature is the first factor that affects the sound speed. Generally, the sound speed of the surface layer and thermocline in the ocean changes significantly, while the temperature of the isothermal layer is relatively stable (Zhao et al., 2019). Seasonal temperature and flow field changes can cause instability of the SSP. Therefore, the SSP has significant temporal and spatial characteristics, and its changes are irregular. Studies have shown that the sensitivity of SSP mismatch to source positioning at different depths is different (Su et al., 2015), so it is necessary to measure the SSP of this area at the same time during underwater positioning measurement (Li, 2015).

The classic ideal Munk-SSP (Figure 2) model is a parametric model of SSP structure. In the past few decades, it has been widely used in related research. It is a classic SSP model suitable for deep-sea areas based on the measured layered characteristics of deep-sea density structure. It is usually expressed by the function $v(z)$ of sound speed v and water depth z (Munk, 1974):

$$v(z) = 1500[1 \cdot 0 + \kappa(\tilde{z} - 1 + e^{-z})] \tag{9}$$

where $\kappa = 0{\cdot}00737$, conversion depth $\tilde{z} = 2(z - 1300)/1300$. When positioning without SSP, the Munk-SSP can be used as a simple replacement, or the global SSP can be constructed based on Argo data (Cai et al., 2014).

The premise of the positioning model based on distance measurement is that the sound speed is a constant, and the trajectory of acoustic rays in the water is a straight line. In order to improve the

https://doi.org/10.1017/S0373463321000400 Published online by Cambridge University Press

efficiency of underwater positioning in the project, based on experience, sometimes the sound speed value is directly taken as 1500 m/s. Obviously, this will bring a large ranging error. When the SSP is measured, the average sound speed based on the SSP is expressed as:

$$V_A = \frac{1}{H}\sum_{i=0}^{N-1}\frac{(V_{i+1}+V_i)(z_{i+1}-z_i)}{2} \tag{10}$$

where H is the water depth, V_i and V_{i+1} are the sound speed values of the i and $i+1$ layer respectively, z_i and z_{i+1} are the depths of the i and $i+1$ layer respectively. The positioning model of the average sound speed method is simple, the calculation method is convenient, and the positioning efficiency is high, but there is still a large residual error.

2.3. The effect of average sound speed on positioning

The acoustic ray, in practice, will bend due to the change of sound speed. Studies have shown that the sound speed determines the accuracy of positioning by affecting the accuracy of ranging. Based on the acoustic ray tracing algorithm, the relationship between ranging and surface sound speed error is derived (Zhao et al., 2019):

$$dL = \frac{k\sin\theta_0}{V_0}\sum_{i=1}^{N}\frac{V_i\Delta z_i}{\sqrt{[1-(kV_i)^2]^3}}dV_0 \tag{11}$$

where k is Snell's constant, L is ranging, θ_0 is the incident angle of surface acoustic rays, V_0 is surface sound speed. It can be seen from Equation (11) that there is a non-linear relationship between the incident angle and the sound speed on the ranging, and the error of the sound speed and the incident angle are positively correlated with the ranging error. The acoustic ray tracing algorithm is a high-precision underwater positioning method commonly used to reduce the acoustic ray bending error (Sakic et al., 2018). When the observed incident angle is large, the average sound speed positioning model and acoustic ray tracing algorithms are used to calculate the horizontal distance of acoustic ray propagation at an incident angle of 85°, the average sound speed is 1470 m/s.

It can be seen from Figure 3 that, when the acoustic signal propagates to the horizontal distance of about 30 m, the difference between the two algorithms begins to appear. When the horizontal distance between the transponder and the source is close to 350 m, under the average sound speed model, the acoustic ray travels to 30 m underwater. While the acoustic ray travels to 70 m under the acoustic ray tracing algorithms, it has a significant impact. In addition, the influence of the average sound speed error on the ranging error under different incident angles is also calculated.

In Figure 4, the sound source depth is 1 m, the incident angle is 30°, 50° and 70°, the average sound speed is 1,470 m/s, and the propagation time is 0·477 s. It can be seen from the experimental results that the horizontal distance reached by the signal propagation under different incident angles is different; The ranging error is affected by the acoustic ray bending error caused by the sound speed error, and it is positively correlated with the incident angle. When the transponder is directly below the sound source, there is no influence of acoustic ray bending error. In addition, the longer the sound signal propagation time, the greater the impact of the sound speed error. Assuming the propagation time is 1 s, the sound speed error of 1 m/s will result in a 1 m ranging error.

The acoustic ray tracing algorithm can effectively reduce the influence of the acoustic ray bending error and restore the footing of the beam more realistically. However, the calculation model of the algorithm is relatively complicated, and the calculation efficiency is lower than that of the average sound speed positioning model, and rapid positioning cannot be achieved. Therefore, it is necessary to consider sound speed correction to reduce the influence of the sound speed error. At present, the main sound speed correction methods include: empirical sound speed method, weighted average sound

https://doi.org/10.1017/S0373463321000400 Published online by Cambridge University Press

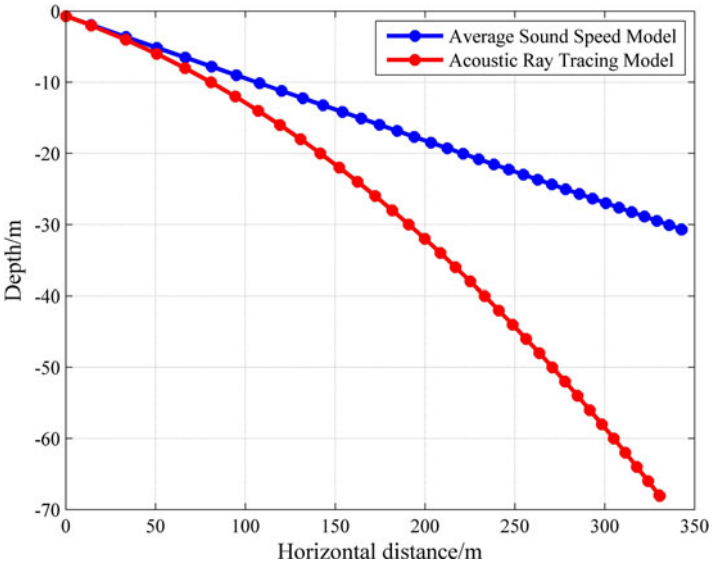


Figure 3. *Influence of average sound speed error.*

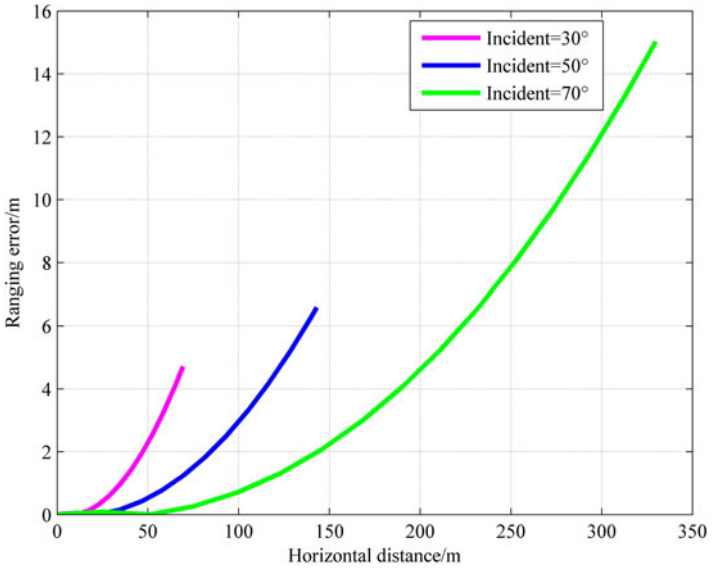


Figure 4. *Effect of average sound speed error on ranging error.*

speed method, Taylor series expansion method, effective sound speed method, equivalent SSP method and acoustic ray tracing algorithm. Due to the limitation of the algorithm, the above method has many applicable conditions, and each has its advantages and disadvantages (Vincent and Hu, 2000; Nie, 2015; Zhang, 2019).

It is easy to obtain from ray theory that when the depth of the target point to be measured is certain, the larger the incident angle, the longer the propagation distance. Therefore, an improved model of incident angle sound speed is considered. On the basis of the traditional average sound speed, the influence of incident angle error is considered, and the calculation complexity is simplified, so as to improve the positioning accuracy while ensuring the calculation efficiency.

https://doi.org/10.1017/S0373463321000400 Published online by Cambridge University Press

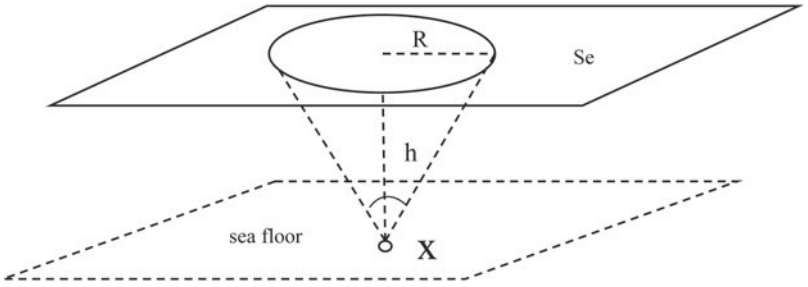


Figure 5. *Absolute calibration navigation positioning.*

3. A new average sound speed model for underwater positioning

Absolute calibration of submarine array is an important task of underwater positioning, which provides strong support for the construction of the submarine array network and the establishment of marine benchmarks (Wu, 2013). In order to weaken the influence of incident angle error as much as possible, the method of circle calibration combined with tracing experiment is usually used to improve the positioning accuracy. Incident angle error includes the error caused by the change of sound speed, the control point error on the sea surface and the propagation time error.

When the sea surface control pattern is a circle (Figure 5), a 'star configuration' has been proposed to eliminate the speed error caused by using different observations, to improve the accuracy of underwater positioning (Xue et al., 2006). Xue (2014) proposed a nested cone configuration and a spiral configuration based on the minimum geometric dilution precision (GDOP) configuration for the expansion of the 'star configuration', and deduced the only five regular polyhedral configurations in mathematics. When the ship's trajectory is approximately circular, the incident angle information is approximately equal, so the influence of the error is minimised. In addition, due to the limited sailing distance of the ship, it can be approximately considered that the SSP used for positioning in a short time is the same. At this time, the influence of the incident angle error can be approximately ignored, and the distance between the shipborne transceiver and the seabed array element is regarded as a straight line, that is, the average sound speed can be used to achieve high-precision positioning (Qi et al., 2019).

Sometimes, however, limited by environmental conditions or positioning requirements in practice, the ship's trajectory on the sea surface is no longer a regular circular symmetrical figure. In this case, the propagation distance of the acoustic ray is different due to the different incident angle, and bending error cannot be ignored due to the influence of sound speed change. If a single sound speed is used, it will cause large positioning error and seriously affect the positioning accuracy. In conclusion, based on the classic Munk-SSP model, a sound speed function model related to the incident angle is established by numerical simulation experiments.

Assume that, under ideal conditions, a series of control points are distributed on a symmetric circle with R radius of the sea surface, and the plane position of the unknown point to be measured is located at the centre of the circle (as shown in Figure 5). Given the water depth of the unknown point to be measured, the incident angle can be calculated iteratively (Wang et al., 2016). The observed incident angle can be obtained by inverse calculation of the coordinates between the sea surface control point and the seabed point to be measured:

$$\theta_i = arc\tan\frac{\sqrt{(x_i^s - x_x)^2 + (y_i^s - y_x)^2}}{||z_i^s - z_x||} \tag{12}$$

where (x_i^s, y_i^s, z_i^s) is the coordinates of the i control point on the sea surface, $(x_x y_x z_x)$ is the coordinates of the point to be measured on the seabed.

https://doi.org/10.1017/S0373463321000400 Published online by Cambridge University Press

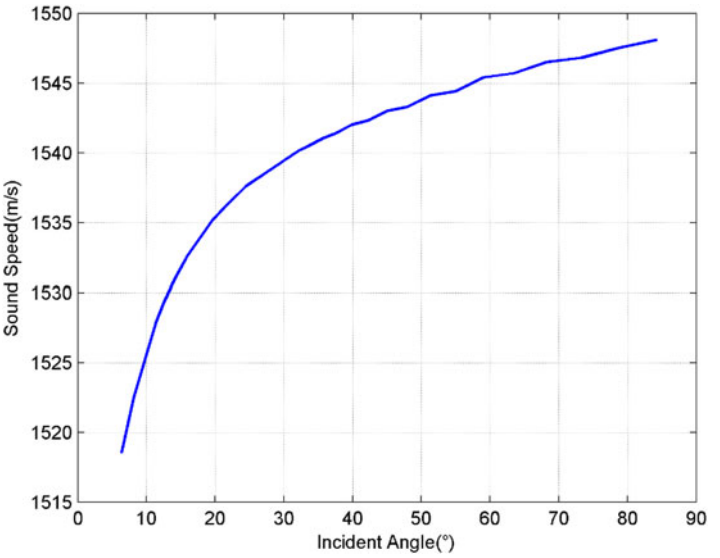


Figure 6. *Relationship between incident angle and sound speed.*

The acoustic ray tracing algorithm is used to simulate the sound signal propagation time t, the average sound speed v is calculated by Equation (10), and the sound speed is multiplied by the time to obtain the ranging for positioning. Keep changing until the best sound speed v' is found, so that the error between the positioning result X_v and the ray tracing positioning result $X_{tracing}$ meets the requirements, $||X_v - X_{tracing}|| \leq \varepsilon$. From this, the optimal sound speed value at a fixed incident angle can be obtained and then, by changing the water depth of the unknown point to be measured to control the incident angle transformation, the relationship between the incident angle and the optimal sound speed can be obtained, as shown in Figure 6. The step length of the incident angle is 2° and the interval is from 8° to 85°.

At this time, the new sound speed positioning model related to the incident angle can be expressed as:

$$\tilde{L}_i = f(v_i) \cdot \mathrm{t}_i + \varepsilon_L \tag{13}$$

where $\tilde{L}$ is the slant distance; t is the propagation time of the acoustic signal; $f(v)$ is a variable function of the sound speed; and the sound speed itself is a function of the incident angle, which can be obtained by fitting the function to Figure 6:

$$f(v_i) = a \cdot {\theta_i}^b + c \tag{14}$$

where a is the scaling factor adjustment factor; b is the constant dependent variable of the power function; c is the constant; θ is the incident angle. According to the numerical simulation test results, the value range of a is [−96·43, −93·29], the value range of b is [−0·4216, −0·3694], and the value range of c is [1562, −1566]. Among them, because the linear relationship between the incident angle and the sound speed is constant, the value range of a and b is unchanged. The premise of this experiment is the Munk-SSP model; there is a difference in the range of sound speed changes compared with different SSP, so the range of c depends on the SSP.

The sum of squares due to error (SSE) represents the sum of squares of errors between the fitted data and the corresponding points of the original data. The closer the SSE is to zero, the better the model selection and fitting, and the more successful the data prediction. The SSE of the model fitting function is 0·8501, indicating that the fitting result is very good. R-square is defined as the ratio of SSR (sum of squares of the regression) to SST (total sum of squares). The closer its value is to one, the stronger the explanatory power of the variables of the equation is for y, and the model fits the data better. The R-square of the fitting function is 0·9995, which can also prove that the fitting accuracy is very high.

https://doi.org/10.1017/S0373463321000400 Published online by Cambridge University Press

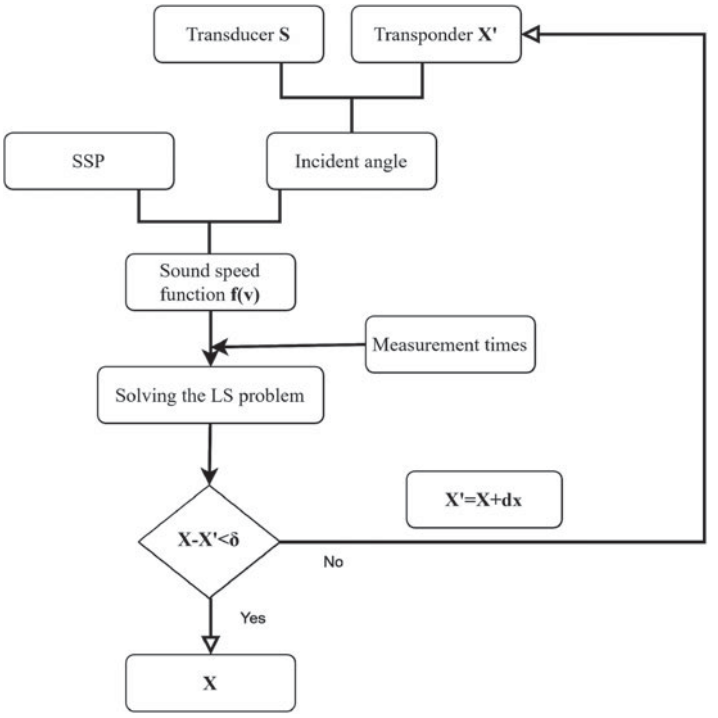


Figure 7. *Positioning flowchart under the new model.*

When the angle of the acoustic ray connecting the sea surface transducer and the transponder to be measured is different, the n incident angles $\boldsymbol{\theta} = [\theta_1, \theta_2, \cdots \theta_n]$ of the acoustic ray can be calculated by Equation (12). Then calculate n corresponding sound speed values $\mathbf{v} = [v_1, v_2, \cdots v_n]$ through Equation (14). When the survey ship performs positioning measurement, it will output n acoustic ray propagation time $\mathbf{T} = [\mathrm{t}_1, \mathrm{t}_2, \cdots \mathrm{t}_n]$ can calculate the ranging $\mathbf{L} = [\mathrm{L}_1, \mathrm{L}_2, \cdots \mathrm{L}_n]$. The symbol '**L**' should be the observed value of multiple ranging, and this ranging refers to the distance between the transponder and the transducer. And then complete the positioning of the underwater target point to be measured according to the distance intersection method. Under this model, when the incident angle changes, the sound speed changes accordingly, which can effectively reduce the influence of the sound speed error on ranging. The above positioning process can be summarised as follows:

In the Figure 7, 'X' represents the coordinate position of the unknown point, and 'X′' represents the least squares solution obtained by using the positioning model proposed in this paper. The algorithm uses an iterative algorithm; when the positioning result does not meet the error requirements, the probability coordinates of the unknown point need to be changed to recalculate the angle of incidence. According to the relationship between the sound speed and the incident angle, a new value of sound speed is obtained, and the new unknown point coordinates are calculated. If $\mathrm{X} - \mathrm{X}' < \delta$, the iterative calculation ends, and the position coordinate 'X' obtained at this time is the true position of the underwater unknown point. The core idea of the new algorithm is given in the form of a program in the Appendix.

4. Experiment analysis

4.1. Simulation experiment and analysis

The simulated trajectory of the ship on the sea surface is a circle with radius $R = 100$ m, the plane position of the unknown target point is at the centre of the circle, and the vertical position is 100 m underwater. Based on Munk-SSP, the ray tracing algorithm is used to simulate the propagation time of

https://doi.org/10.1017/S0373463321000400 Published online by Cambridge University Press

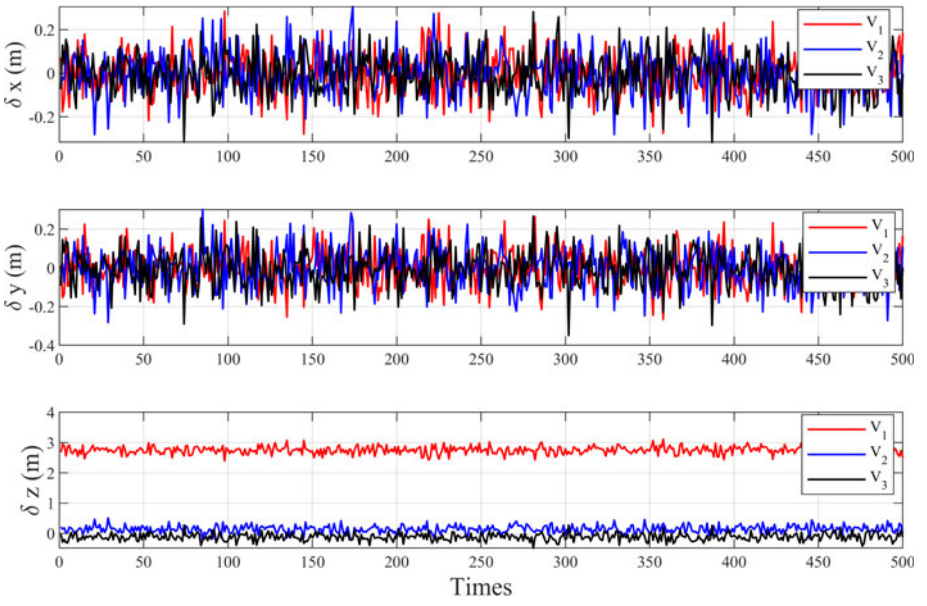


Figure 8. *Underwater geometric positioning errors caused by three sound velocity models under the same incident angle.*

the acoustic signal. The simulated sea surface is a cosine wave with a wave height of 2 m, the measured ship speed is 3 kn/h, the sampling interval is 4 s, and the ranging error is 0·3% times the slope distance (Zhao et al., 2018). The positions of the seafloor target in simulation test are known, so it is possible to compare the accuracy of positioning results of different models.

Three different sound speed determination methods are used for positioning experiments. The first model is the average sound speed of Munk-SSP, that is, $V_1 = \text{mean}[\text{SSP(v)}]$. The second model is based on the positioning results of the ray tracing algorithm, that is, $V_2 = \text{tracing}(SSP)$. The core idea of the ray tracing algorithm is given in the form of a program in the Appendix. The third model is to use the new sound speed positioning model related to the incident angle $V_3(\theta)$ proposed in this paper; its calculation flow is shown in Figure 7. The positioning experiment was repeated 500 times, and the deviation sequence and variance of different positioning models and true values were counted to evaluate the reliability of the results.

Several conclusions can be seen from the experimental results in Figure 8 and Table 1:

1. When the average sound speed model V_1 is used for positioning, since the sea surface control graphic is a symmetrical circle, the positioning accuracy in the plane direction is high, and the error with the real position of the target is small. The positioning error of the average sound speed model is mainly reflected in the vertical direction, because the water surface control points are approximately coplanar, resulting in an ill state in the vertical direction, so the vertical positioning accuracy is poor.
2. When the ray tracing model V_2 is used for positioning, it can be seen that the positioning result is very close to the real position of the target. The reason is that the observation configuration is symmetrical, the incident angle is approximately equal, and the incident angle error affects the positioning accuracy through the ranging error.
3. When the new positioning model $V_3(\theta)$ is used for positioning, it can be seen that the deviation between the positioning result and the real position in the three directions is very small, and it is similar to the ray tracing model. The reason is that the sound speed used to calculate the distance measurement is no longer a single sound speed value, but a function related to the incident angle.
4. Compared with the average sound speed positioning model, the new positioning model related to the incident angle improves the vertical positioning accuracy. Compared with the ray tracing model,

https://doi.org/10.1017/S0373463321000400 Published online by Cambridge University Press

Table 1. *Variance of positioning results under different models.*

Model	Variance		
	X	Y	Z
V_1	0·0099	0·0097	0·0163
V_2	0·0095	0·0098	0·0150
$V_3(\theta)$	0·0098	0·0096	0·0152

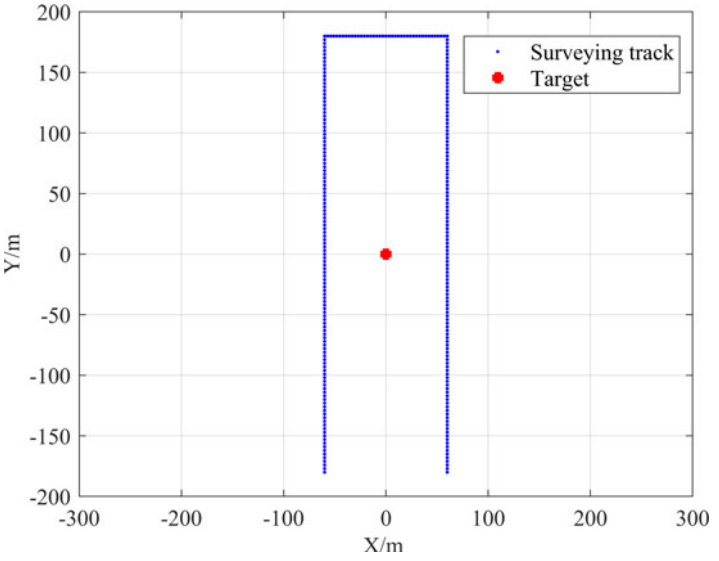


Figure 9. *Rectangular surveying track.*

the positioning accuracy is equivalent under the symmetrical circle control graph; when the sea surface control graphics is not a circularly symmetrical graph, the advantages of the new model will be reflected, and the authors will verify this conclusion in subsequent experiments.

In addition, a simulation experiment was conducted with different incident angles. The surveying track of the simulated ship on the sea is a rectangle, and the error simulation method is the same as the above simulation experiment. The surveying track of the ship on the sea is shown in Figure 9, 'Target' indicates the position of the underwater target point.

Correspondingly, according to the change of the incident angle, the corresponding sound speeds are calculated by Equation (14), and the relationship between them is shown in Figure 10.

Similar to the above simulation experiment, three different positioning models are used for calculation. V_1 is the average sound speed positioning model, V_2 is the ray tracing positioning model, and V_3 is the new sound speed positioning model. The positioning error is shown in Figure 11.

Through the experimental results, we can see that the V_1 model has poor positioning accuracy in three directions for the observations with the unequal incident angles. The reason is that a fixed sound speed is used for positioning. The positioning accuracy of the V_2 and V_3 models perform better than V_1, and the overall conclusion is the same as the above simulation test with the equivalently incident angles.

In summary, whether it is a circular calibration experiment or a positioning experiment with irregular observation patterns, the new positioning model related to the incident angle can quickly achieve high-precision underwater positioning.

https://doi.org/10.1017/S0373463321000400 Published online by Cambridge University Press

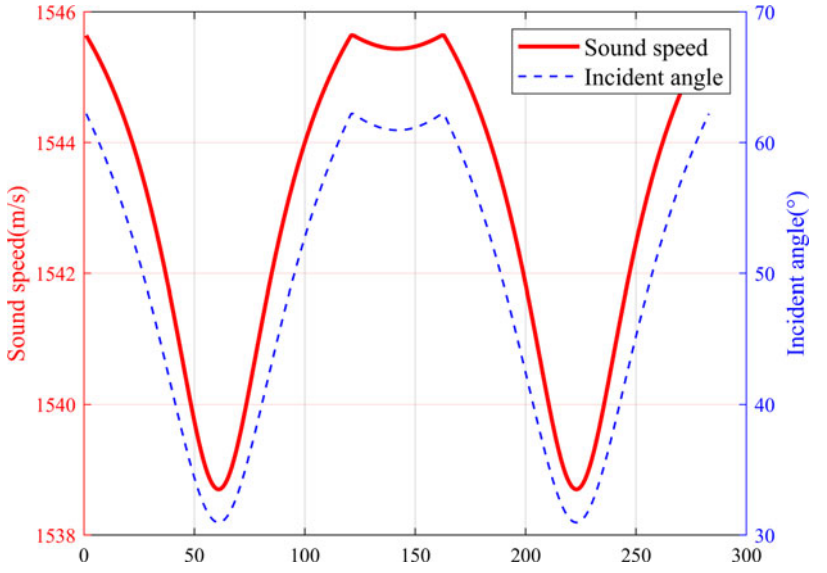


Figure 10. *Relationship between sound speed and incident angle.*

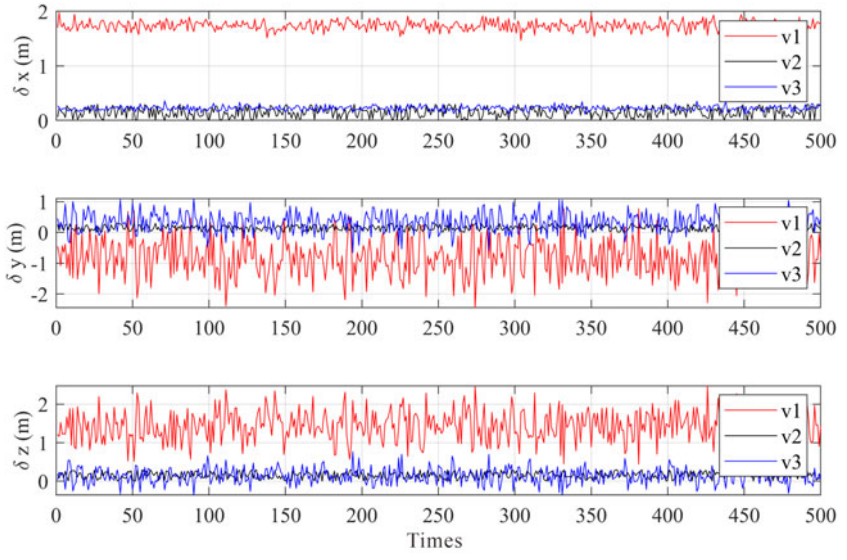


Figure 11. *Underwater geometric positioning errors caused by three sound velocity models under different incident angles.*

4.2. Real experiment and analysis

In order to verify the validity of the new positioning model related to the incident angle proposed in this paper, relevant actual measurement experiments were carried out. The positioning experiment was carried out in October 2012 on a lake in northern China, with a total area of about 554 km^2 and maximum water depth of about 77 m. The target transponder was about 60 m underwater. The main equipment required for the experiment were: a measurement ship equipped with Leica GPS1200 dual-frequency real-time kinematic (RTK), vertical reference unit (VRU), Gyroscope (Gyro), long-base line (LBL) positioning system, sound velocity profile (SVP), data processing centre, etc. The LBL system used Sonardyne's 6G LBL acoustic positioning system. The ship's attitude sensor model was Seatex

https://doi.org/10.1017/S0373463321000400 Published online by Cambridge University Press

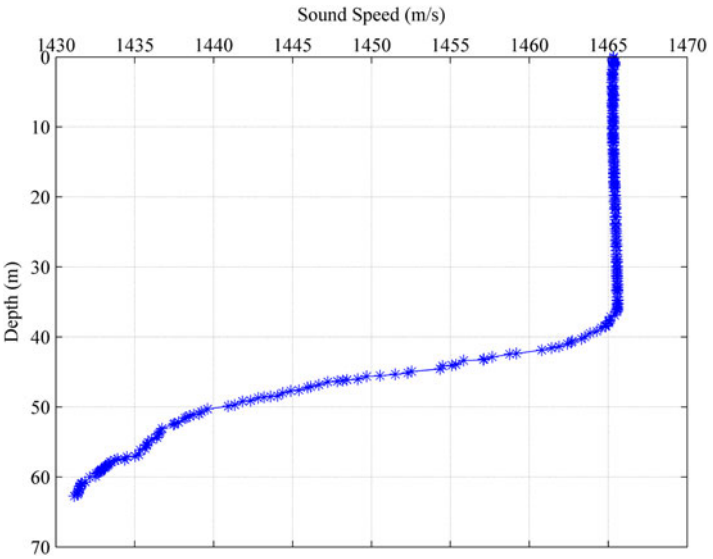


Figure 12. *Sound speed profile of the survey area.*

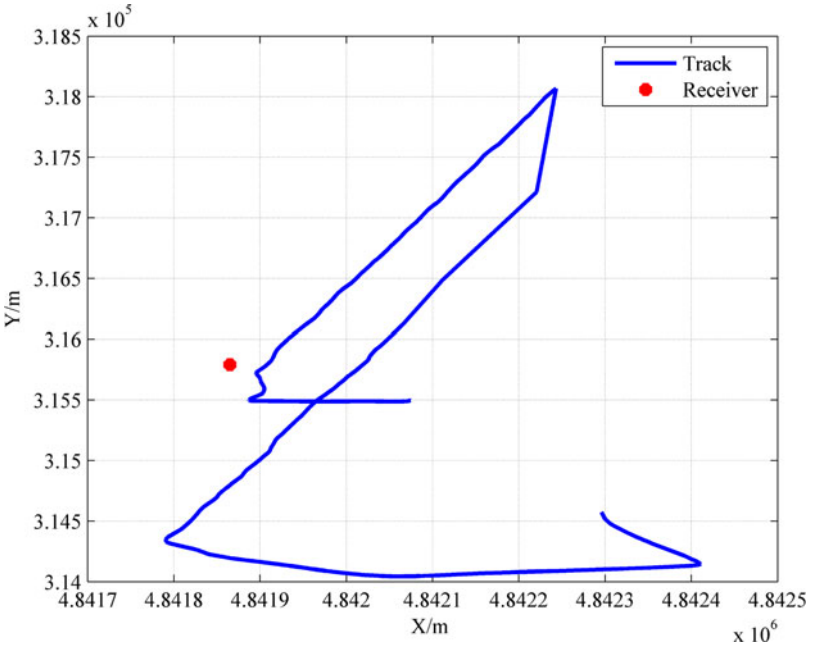


Figure 13. *Survey ship's trajectory and the position of the receiver.*

MRU-05, with roll/pitch measurement accuracy of ±0·05° and heave accuracy of ±5 cm. The underwater sound speed meter used AML SVP to measure the SSP of the water area Figure 12.

The experiment used track navigation and positioning, that is, the measuring ship did not follow a regular shape on the water surface, and the observation values at different incident angles were obtained. The sailing track is shown in Figure 13.

According to the initial value of the transponder position and the coordinates of the dynamic control point of the measuring ship, the incident angles of different observations can be inversely calculated, and then the new sound speed positioning model $V_3(\theta)$ can be calculated by Equation (14); at the same

https://doi.org/10.1017/S0373463321000400 Published online by Cambridge University Press

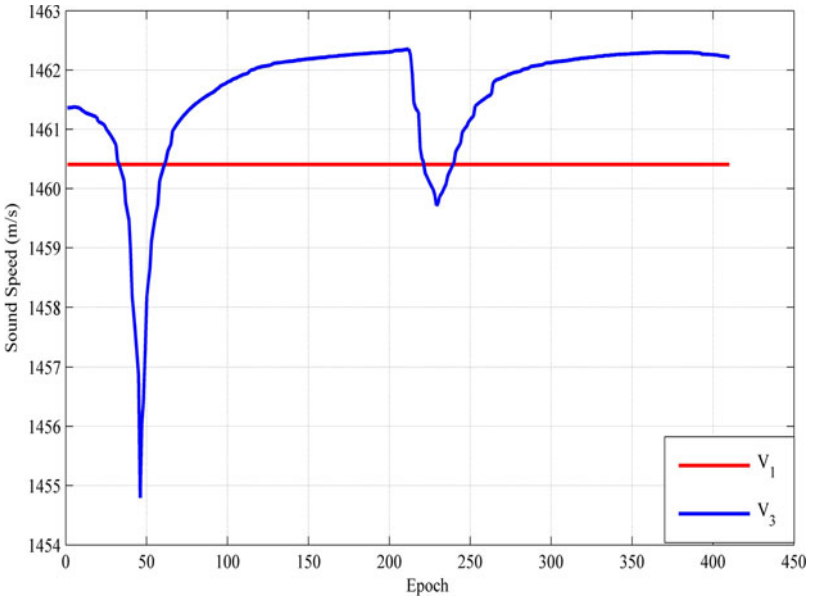


Figure 14. *Comparison of two sound speeds.*

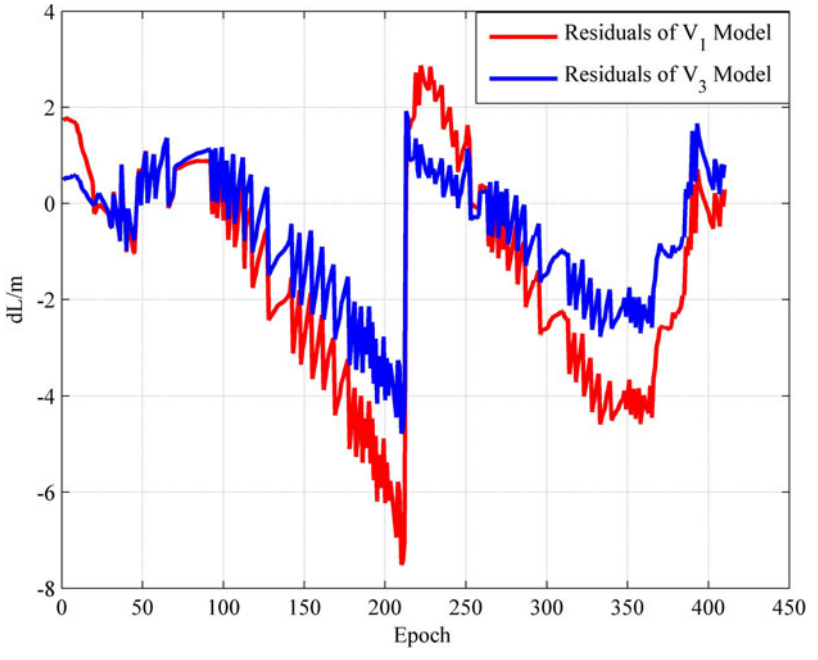


Figure 15. *Comparison of residuals of two positioning results under two models.*

time we give the average sound speed V_1. Figure 14 shows the comparison of the relationship between the two sound speed values.

Positioning results were performed under two different models. The residual information contains important information about the basic assumptions of the model, and the residual relationship under the two positioning results is given (Figure 15).

https://doi.org/10.1017/S0373463321000400 Published online by Cambridge University Press

Table 2. *Deviation of positioning results under different models: unit (m).*

Positioning deviation	ΔX	ΔY	ΔZ	PE
V_1 model	3·9726	1·0354	−2·8276	4·9848
$V_3(\theta)$ model	0·9826	0·2527	−0·4823	1·1233

It can be seen from the positioning residuals of the two positioning models that the residuals of the new sound speed positioning model $V_3(\theta)$ are generally smaller than the average sound speed positioning model V_1. The reason is that the $V_3(\theta)$ is used instead of a single sound speed value V_1, which releases the residual information, reduces the influence of the sound speed error on the positioning, and improves the accuracy of parameter estimation.

In addition, it was noticed that there is a significant mutation for positioning residuals approximately at the 210th epoch. Combined with the navigation route in Figure 12, and through the position relationship between the transducer and the underwater transponder, the authors believe that at the 210th epoch the ship sailed to the farthest point, and then the route and direction of sailing changed, where the incident angle and other related errors have the greatest impact.

Taking the acoustic ray tracing positioning result as the true value, Table 2 shows the deviation of the positioning results in three directions under different models. From the results, the results of the $V_3(\theta)$ model in the three directions are closer to the results of acoustic ray tracing, and the positioning accuracy has been greatly improved. The three directions of X, Y, and Z are raised by about 3 m, 0·8 m and 2·4 m, respectively. From the positional error (PE) value, $PE = \sqrt{(\Delta X)^2 + (\Delta Y)^2 + (\Delta Z)^2}$, the PE values under the two models are 4·9848 and 1·1233, respectively. It is obvious that the $V_3(\theta)$ model is effective.

5. Conclusion

Based on the introduction of the average sound speed positioning model, this paper discusses the influence of sound speed error on positioning accuracy. Combined with the actual situation, considering the influence of the error related to the incident angle, a new sound speed positioning model related to the incident angle is established to replace the single sound speed value in the average sound speed model for positioning. The following conclusions were obtained through simulation experiments and actual measurement experiments:

(1) The error of sound speed is an important source which affects the accuracy of underwater positioning and cannot be ignored. Sound speed error affects the ranging and causes the positioning result to be inaccurate. Therefore sound speed correction is required for high-precision underwater positioning.
(2) Considering the impact of incident angle related errors on positioning, this paper proposes a new sound speed positioning model related to the incident angle to reduce the model error. Through experiments, the average sound speed model has a large positioning error due to the incident angle error, especially in deep water and long-distance positioning. The new sound speed positioning model related to the incident angle proposed in this paper is used for positioning, and it shows good positioning performance when the observation graph is circular or non-circular.
(3) The starting point of the new positioning model proposed in this paper is to fit a positioning model with a small number of acoustic rays. Once the model is established, when the user performs repeated positioning in a certain area, it does not need to repeat the complicated acoustic ray tracing positioning calculations, but only needs to calculate a correction value according to the new model, and the positioning can be realised quickly based on this correction value. It can reduce the cost of calculation on the basis of ensuring the positioning accuracy, which is convenient for users.

Funding statement. This study was supported by the National Natural Science Foundation of China (No. 41931076), Major Science and Technology Innovation Projects of Shandong Province (No. 2019JZZY010809).

https://doi.org/10.1017/S0373463321000400 Published online by Cambridge University Press

References

Cai, Y. and Cheng, P. (2012). Sound velocity problem of undersea positioning in up ocean. *Remote Sensing Information*, **027**(006), 3–9.

Cai, Y. H., Cheng, P. F., Wen, H. J., Yang, X. X. and Zhang, J. D. (2014). Study on global sound speed field of seawater using ARGO profile data. *Remote Sensing Information*, **29**(5), 13–19.

Fujita, M., Ishikawa, T., Mochizuki, M., Sato, M., Toyama, S. I., Katayama, M., Matsumoto, Y., Yabuki, T. and Asada, A. (2006). GPS/acoustic seafloor geodetic observation: Method of data analysis and its application. *Earth, Planets and Space*, **58**(3), 265–275.

Jamshidi, S. and Abu Bakar, M. N. (2010). Temperature, salinity and density measurements in the coastal waters of Rudsar, south Caspian Sea.*Discover the World's Research*, **1**(1), 27–36.

Li, S. (2015). *Research on the Method of Sound Speed Correction in Underwater Acoustic Positioning*. Qingdao, China: China University of Petroleum.

Liu, Y., Xue, S., Qu, G., Lu, X. and Qi, K. (2020). Influence of the ray elevation angle on seafloor positioning precision in the context of acoustic ray tracing algorithm. *Applied Ocean Research*, **105**, 102403.

Munk, W. H. (1974). Sound channel in an exponentially stratified ocean, with application to SOFAR. *Journal of the Acoustical Society of America*, **55**(2), 220–226.

Nie, Z., Wang, Z. and Li, S. (2015). Comparison of sound speed correction methods in the underwater acoustic positioning. *Marine Science Bulletin*, **34**(4), 66–70.

Qi, K., Qu, G. Q., Xue, S. Q., Xu, T. H. and Su, X. Q. (2019). Analytical optimization on GNSS buoy array for underwater positioning. *Acta Oceanologica Sinica*. (7), 137–143.

Sakic, P., Ballu, V., Crawford, W. C. and Woeppelmann, G. (2018). Acoustic ray tracing comparisons in the context of geodetic precise off-shore positioning experiments. *Marine Geodesy*, **41**(4), 315–330.

Su, L., Ma, L., Song, W. H., Guo, S. M. and Lu, L. C. (2015). Influences of sound speed profile on the source localization of different depths. *Acta Physica Chinese Edition*, **64**(2), 24302-024302.

Sun, W. (2007). *Studies on Underwater Acoustic Localization Technique in Shallow Water and Its Application*. Qingdao, China: Ocean University of China.

Vincent, H. T. and Hu, S. L. J. (2000). Generalized Multivariate Error Propagation for Zero Memory Nonlinear Systems. *Proceedings of 8th ASCE Specialty Conference on Probabilistic Mechanics and Structural Reliability*.

Wang, Y., Li, W., Liang, G. and Fu, J. (2009). The Influence and Revision of Ray Bending in Synchronous Underwater Acoustic Positioning System. *Proceedings of the 2009 Youth Academic Conference CYCA'09 of the Acoustic Society of China*.

Wang, Z., Li, S., Nie, Z., Wang, Y. and Wu, S. (2016). A large incidence angle ray-tracing method for underwater acoustic positioning. *Geomatics and Information Science of Wuhan University*, **41**(10), 1404–1408.

Wu, Y. (2013). *Study on Theory and Method of Precise LBL Positioning and Development of Positioning Software System*. Wuhan, China: Wuhan University.

Xue, S. and Yang, Y. (2014). Nested cones for single-point-positioning configuration with minimal GDOP. *Geomatics & Information Science of Wuhan University*, **39**(11), 1369–1374.

Xue, S., Dang, Y. and Zhang C. (2006). Research on setting 3D network of underwater DGPS. *Science of Surveying and Mapping*, **31**(4), 23–24.

Yang, Y., Liu, Y., Sun, D., Xu, T. and Zeng, A. (2020). Seafloor geodetic network establishment and key technologies. *Science China Earth Science*, **63**, 1188–1198.

Zhang, B. (2019). *Research on High Precision Positioning Algorithm for Underwater Acoustics*. Chang'an, China: Chang'an University.

Zhao, J. and Liang, W. (2019). Some key points of submarine control network measurement and calculation. *Acta Geodaetica et Cartographica Sinica*, **48**(9), 1197–1202.

Zhao, J. and Liu, J. (2008). *Multi-Beam Bathymetry and Image Data Processing*. Wuhan, China: Wuhan University Press.

Zhao, J., Li, J. and Li, M. (2009). Progress and future trend of hydrographic surveting and charting. *Journal of Geomatics*, **34**(4), 25–27.

Zhao, D., Liu, X., Zhao, H. and Wang, C. (2020). Seamless integration of polarization compass and inertial navigation data with a self-learning multi-rate residual correction algorithm. *Measurement*, **170**(3), 18694.

Zhao, S., Wang, Z. and Liu, H. (2018). Investigation on underwater positioning stochastic model based on sound ray incidence angle. *Acta Geodaetica et Cartographica Sinica*, **77**, 69–77.

https://doi.org/10.1017/S0373463321000400 Published online by Cambridge University Press

A. APPENDIX

Algorithm 1. *Ray tracing algorithm.*

While
Start with travelling time.
for $i = 1$ to N **do**
$$t_i(\boldsymbol{x}) = \int_{L(\boldsymbol{x}^i,\boldsymbol{x})} \frac{ds}{v} = \int_{h_i}^{h_x} \frac{dh}{v(h)\cos\alpha}$$
end for
Next
for $j = 1$ to N **do**
$L_j = norm(X_j - X_0)$
$B_j = (X_0 - X_j)/L_j$
end for
Compute the residual:
$dL = Speed * T - Speed * t$
Compute the least square solution:
$dX = inv(B' * B) * B' * dL'$
Location update:
$X' = X_0 + dX$
if $X' - X_0 < \varepsilon$
end if
end while

Algorithm 1: Location algorithm based on new model
Compute the incident angle at first:
$$\theta_i = arc\tan\frac{\sqrt{(x_i^s - x_{\mathrm{x}})^2 + (y_i^s - y_{\mathrm{x}})^2}}{||z_i^s - z_{\mathrm{x}}||}$$
Start with SSP and incident angle.
While
Compute the sound speed function:
$f(v_i) = a \cdot {\theta_i}^b + c$
Compute the geometrical distance:
$\tilde{L}_i = f(v_i) \cdot \mathrm{t}_i + \varepsilon_L$
The travelling time is obtained by measurement.
Next
Compute the least square solution:
$dX = inv(B' * B) * B' * dL'$
Location update:
$X' = X_0 + dX$
if $X' - X_0 < \varepsilon$
end if
end while

Cite this article: Liu Y, Lu X, Xue S, Wang S (2021). A new underwater positioning model based on average sound speed. *The Journal of Navigation* **74**: 5, 1009–1025. https://doi.org/10.1017/S0373463321000400

https://doi.org/10.1017/S0373463321000400 Published online by Cambridge University Press